1-16-2008

Influence of Morphology and Permafrost Dynamics on Hyporheic Exchange in Arctic Headwater Streams under Warming Climate Conditions

Jay P. Zarnetske
Utah State University

Michael N. Gooseff
Pennsylvania State University

W. Breck Bowden
University of Vermont

Morgan J. Greenwald
University of Vermont

Troy R. Brosten
Boise State University

See next page for additional authors

Authors

Jay P. Zarnetske, Michael N. Gooseff, W. Breck Bowden, Morgan J. Greenwald, Troy R. Brosten, John H. Bradford, and James P. McNamara

Click Here for Full Article

Correction published 28 February 2008

Influence of morphology and permafrost dynamics on hyporheic exchange in arctic headwater streams under warming climate conditions

Jay P. Zarnetske,[1] Michael N. Gooseff,[2] W. Breck Bowden,[3] Morgan J. Greenwald,[3] Troy R. Brosten,[4] John H. Bradford,[4] and James P. McNamara[4]

[1] We investigated surface-subsurface (hyporheic) exchange in two morphologically distinct arctic headwater streams experiencing warming (thawing) sub-channel conditions. Empirically parameterized and calibrated groundwater flow models were used to assess the influence of sub-channel thaw on hyporheic exchange. Average thaw depths were at least two-fold greater under the higher-energy, alluvial stream than under the low-energy, peat-lined stream. Alluvial hyporheic exchange had shorter residence times and longer flowpaths that occurred across greater portions of the thawed sediments. For both reaches, the morphologic (longitudinal bed topography) and hydraulic conditions (surface and groundwater flow properties) set the potential for hyporheic flow. Simulations of deeper thaw, as predicted under a warming arctic climate, only influence hyporheic exchange until a threshold depth. This depth is primarily determined by the hydraulic head gradients imposed by the stream morphology. Therefore, arctic hyporheic exchange extent is likely to be independent of greater sub-stream thaw depths. **Citation:** Zarnetske, J. P., M. N. Gooseff, W. B. Bowden, M. J. Greenwald, T. R. Brosten, J. H. Bradford, and J. P. McNamara (2008), Influence of morphology and permafrost dynamics on hyporheic exchange in arctic headwater streams under warming climate conditions, *Geophys. Res. Lett.*, *35*, L02501, doi:10.1029/2007GL032049.

1. Introduction

[2] Stream-subsurface exchange within the hyporheic zone is a fundamental process that affects the biogeochemistry [*Jones and Mulholland*, 2000] and residence time [*Haggerty et al.*, 2002] of stream water. The hyporheic zone is an important component of stream ecosystems and most of the understanding of related processes has come from studies of temperate streams. Recently, *Edwardson et al.* [2003] provided an initial documentation of arctic stream hyporheic processes indicating that hyporheic nutrient re-generation may be important because nutrients are extremely limited in most arctic streams.

[3] In temperate stream systems, the dominant driver of hyporheic exchange is the distribution of head gradients, established by stream bed topography, which drives advective flow into and out of the stream bed [*Harvey and Bencala*, 1993]. In arctic streams, climate-driven permafrost and river ice impact channel morphology and bed ice conditions [*Best et al.*, 2005]. Consequently, advective hyporheic processes are likely controlled by ice-influenced channel morphology and sediment conditions. Similar to temperate streams, climate also dictates many of the physical conditions under which arctic stream morphologies develop (e.g., snow-melt dominated hydrographs), except that climate has also led to the development and dynamic nature of the active-layer. Permafrost underlies an active-layer of thawed sediment that develops and increases downward (e.g., as much as 0.2 to >1.0 m in vegetated tundra landscapes) during the summer thaw period from May to September [*Osterkamp and Romanovsky*, 1999].

[4] When the streambeds thaw seasonally, there is a potential for hyporheic exchange to occur. Recent sub-stream thaw investigators [*Bradford et al.*, 2005] observed much greater depths of thaw under stream channels than under the adjacent terrain, suggesting that streams cause preferential thaw. *Brosten et al.* [2006], found that the active-layer beneath low-energy streams (i.e., shallow stream gradients) responded slowly to seasonal energy input and maintained thaw depths longer throughout the late season, whereas the seasonal thaw depths beneath high-energy streams increased and decreased rapidly at the beginning and end of the thaw season. Warming of the arctic climate is expected to result in more persistent thaw seasons causing thicker active-layer conditions and warming of surface waters [*Osterkamp and Romanovsky*, 1999]. Thus thaw layers under stream channels will likely deepen and persist over longer periods of time under a warmer arctic climate.

[5] Our goal was to characterize the current influence of sub-stream thaw depth on hyporheic exchange dynamics in arctic streams, as well as the influence of greater thaw depths predicted under a warmer climate. Previous efforts toward this goal were complicated by the presence of many hyporheic system controlling variables (e.g., dynamic discharges and active layers) [*Zarnetske et al.*, 2007]. Consequently, we have designed a modeling investigation to distinguish the effects of thaw depth from channel morphology. We used empirical results derived from tracer experiments and measurements of sub-stream thaw, hydrau-

[1]Department of Watershed Sciences, Utah State University, Logan, Utah, USA.
[2]Department of Civil and Environmental Engineering, Pennsylvania State University, University Park, Pennsylvania, USA.
[3]Rubenstein School of the Environment and Natural Resources, University of Vermont, Burlington, Vermont, USA.
[4]Department of Geosciences, Boise State University, Boise, Idaho, USA.

lic, and channel morphology conditions to inform ground-water flow and particle tracking models. These types of models have been successfully used to investigate hyporheic exchange elsewhere [e.g., *Kasahara and Wondzell*, 2003; *Saenger et al.*, 2005]. Here we specifically assess hyporheic flowpath extents and cumulative distributions of residence times for simulated particles moving through the hyporheic zone (CDRTs) under a variety of sub-stream thaw conditions.

2. Methods

2.1. Study Site

[6] Two study streams, an alluvial and a peat-lined reach, are located in the northern tundra foothills of the Brooks Range, Alaska (68°38′N, 149°38′W) and are underlain by continuous permafrost with a seasonally dynamic thaw layer [*Brosten et al.*, 2006]. The alluvial reach (AS) is 188 m long, with a cobble and sand bed, moderately steep (0.7%), shallow, single-thread, pool-riffle morphology. The peat-lined reach (PS) is 175 m long, with a shallow (0.03%), deep and narrow, single-thread, beaded channel morphology. The reaches are separated by <0.5 km and are in the Kuparuk River drainage, which runs north to the Arctic Ocean. These reaches represent the two dominant morphologic types of headwater streams found in this region of the Arctic (for more detail see *Zarnetske et al.* [2007] and references therein).

2.2. Measurements

[7] Solute injection experiments (SIEs) were conducted twice at each stream site during the summer of 2005. Rhodamine WT (Turner Designs, Sunnyvale, CA), was injected at a constant rate to the head of each study reach until a stable in-stream tracer concentration was achieved at the base of the reach, as determined by real-time, in-stream monitoring with a field fluorometer (SCUFA, Turner Designs).

[8] Prior to the SIEs, multilevel streambed sampler nests were deployed in both reaches to collect subsurface water [*Greenwald*, 2007]. Sampler nests were placed in the dominant longitudinal channel morphologic units (e.g., riffle head). In total, 9 nests, each with 3 samplers at staggered depths, were installed in AS, in each unit type - riffle heads, riffle tails, and pools, to depths between 11 and 136 cm. PS had 9 nests, each consisting of two samplers, in each unit type - run heads, run tails, and pools, to depths between 10 and 42 cm (Table S1 of the auxiliary material[1]). Tracer samples were collected in the surface flow and from all subsurface samplers at regular intervals throughout the SIEs. All samples were analyzed in a laboratory with a 10-AU fluorometer (Turner Designs) within 3 days of collection.

[9] Alluvial SIEs occurred on 18 June and 8 August and PS SIEs occurred on 27 June and 11 August 2005. All four SIEs were executed under low flow conditions. From the tracer break through curve at each sampler, we computed median observed arrival times, t_{MEDOBS},[2] as half the time

interval from the initial tracer arrival to the peak tracer concentration for any given sampler location.

[10] We collected detailed thalweg surface water and bed surface topography data in June 2005 for both reaches using a Topcon (Model GTS-226) total station and standard surveying methods with spatial resolution of x ≤ 1 m, y ≤ 1 m, z ≤ 0.01 m. Stream sediment hydraulic conductivities for each reach stream unit (*n* = 8 per unit) were determined with the Hvorslev falling-head slug method [*Freeze and Cherry*, 1979].

[11] We used ground penetrating radar (GPR) profiles to estimate the depth of thaw in and adjacent to both reaches. Following the methods by *Brosten et al.* [2006], we collected two-dimensional (2-D) GPR surveys across pool, riffle, and run units at fixed cross-sections in both reaches. These surveys provided estimates of reach-average thaw depths for each stream unit.

2.3. Model Simulations

[12] The numerical groundwater flow model MODFLOW was used to simulate 2-D flow in the stream substrate. Our use of a 2-D longitudinal representation of the stream is appropriate within the context of previous modeling efforts [*Harvey and Bencala*, 1993; *Kasahara and Wondzell*, 2003], which demonstrated that longitudinal discontinuities in the stream profile dominate hyporheic exchange in headwater streams. Furthermore, permafrost is assumed to limit lateral exchange in the subsurface. The model domain represents the longitudinal channel cross section of the thalweg for each study reach (Figure 1). Each model was partitioned into 0.5 m longitudinal columns with an additional 10 m of simplified stream length (i.e., the bed surface was linear and set equal to the measured streambed surface gradient) added to the top and bottom of each reach to reduce the influence of upstream and downstream boundary conditions. The subsurface was divided into 7 layers, with thicknesses appropriate to generate cells matching the vertical resolution of discrete subsurface samplers. The streambed elevations were imported from the topographic survey. A constant head boundary condition, established by the measured surface water elevations, was assigned to the top layer in the models, and a basal no-flow boundary condition simulated the presence of permafrost beneath the lowest layer. The thawed layer thickness was defined by the appropriate June or August GPR survey for riffles, runs, and pools. For all sediment layers, anisotropy of hydraulic conductivity (K) was incorporated such that K_X (horizontal) was an order of magnitude greater than K_Z (vertical) [*Freeze and Cherry*, 1979]. Groundwater and lateral surface inflow or outflow was considered negligible and was not incorporated into the model design because these stream reaches are effectively bound by permafrost (no observed thaw expansion below the banks) and had negligible observed lateral flow exchange. However, future observations of subsurface dynamics may alter these model design assumptions, and require the use of alternative models (e.g., a 3-D model domain).

[13] Three distinct K zones (riffle head, riffle tail, and pool) were longitudinally distributed along the AS model, and only two K zones were incorporated into the PS model, because field K values indicated no difference in the hydraulic properties between run head and run tail units.

---

    [2]The mathematical terms t_{MEDOBS}, K_X, K_Z, t_{MEDSIM}, A_{HZ}*, $A_{HZ,i}/A_{HZ,max}$, A_{HZ}, $A_{TD,i}$, L^{-1}, Ls^{-1}, $m\ s^{-1}$, and t_{HZ} have been corrected here and throughout. The article as originally published is online.
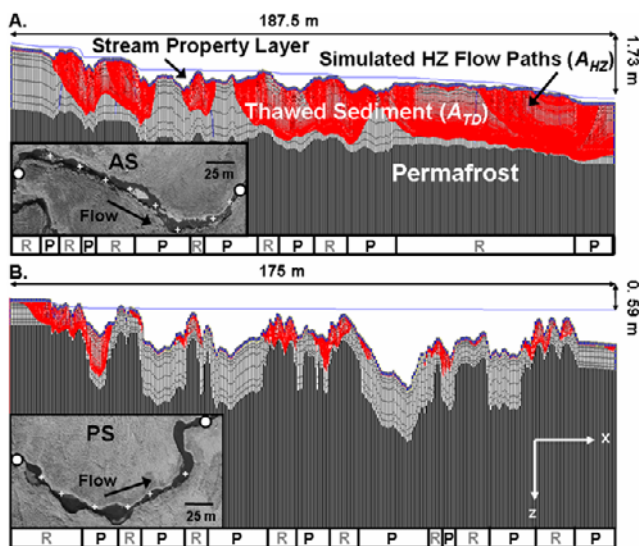
Figure 1. Schematics of (a) the alluvial (AS) and (b) the peat-lined (PS) reaches for the August model domain and design showing stream surface elevation and simulations of the hyporheic particle flow paths and area (A_{HZ}). For brevity, only the August cases are presented. Note: vertical exaggeration is 10:1, dark-grey region is permafrost, and light-grey is thawed substrate (A_{TD}). The channel morphologic units of the domain are shown by "P" for pools and "R" for riffles (Figure 1a) or runs (Figure 1b). Inset aerial photos have dots signifying the top and bottom of a study reach, and cross-hairs representing hydraulic conductivity measurement locations.

MODFLOW coupled with MODPATH particle tracking models were then calibrated by simulating water particle transport time from observation cell to bed surface cells (median arrival time of 40 particles, t_{MEDSIM}). These results were then compared to the observed tracer transport time (median arrival time, t_{MEDOBS}, defined in section 2.2) for each sampler, using the mean empirical K values as initial conditions (AS K = 0.016 m s^{-1} and PS K = 0.002 m s^{-1}). Porosity for AS and PS models were 0.3 and 0.2, respectively. Each K zone value was varied until a minimum root mean squared error between observed and simulated travel times was achieved.

[14] In each calibrated model of June and August conditions, the maximum allowable number of particles (16) was assigned at the top of all uppermost sediment cells (i.e. the stream bed surface). MODFLOW and MODPATH simulations were then run to steady-state for June and August models. The August models for both reaches were modified to assess deeper thaw scenarios, because they represent the maximum observed thaw depths for 2005. The influence of different thaw depths was explored by either compressing or expanding the thawed sediment layer thickness above the permafrost. Eight different simulations were run for each stream, ranging from 25–200% of the observed August thaw depth condition.

[15] An inter-scenario and inter-site comparison of the spatial hyporheic development of sub-channel thaw region was conducted, where flowpaths that originated and terminated at the streambed defined the hyporheic zone. For this spatial hyporheic analysis, the dimensionless area of hyporheic exchange, A_{HZ}*, for each simulation (i) was determined as $A_{HZ,i}/A_{HZ,\max}$, where A_{HZ} is the measured longitudinal cross-sectional area with hyporheic exchange for a simulation, and $A_{HZ,\max}$ is the maximum A_{HZ} calculated across all simulations for a reach (see Figure 1). Furthermore, the ratio of $A_{HZ,i}$ to $A_{TD,i}$, where A_{TD} is the longitudinal cross-sectional area of the thawed depth, facilitated both inter-scenario and -site evaluations of hyporheic development.

3. Results

3.1. Field Conditions and Experiments

[16] The depths of thaw under both streams increased from June to August. Under AS, the average thaw depths were 1.21 m under riffles and 1.26 m under pools (29 June 2005). These thicknesses increased to 1.83 m under both riffles and pools by 5 August 2005. Under PS, the average thaw depth under the runs was 0.40 m on 28 June 2005 and 0.60 m on 4 August 2005, and under the pools thaw depth increased from 0.68 to 0.97 m from June to August.

[17] The AS 18 June and 3 August 2005 injections occurred for 2.63 and 2.33 hr, respectively, in-stream tracer plateau conditions were 40.5 and 45.3 μg L^{-1}, and the measured discharges were 31 Ls^{-1} and 25 Ls^{-1}, respectively. The PS SIE injection periods were 6.00 and 9.77 hr for 27 June and 11 August 2005, respectively, and had instream tracer plateaus of 86.3 and 122.7 μg L^{-1}, respectively. Discharges in the PS were 24 L s^{-1} in June and 20 L s^{-1} in August. Stream water temperatures differed <3.0°C between injections for each reach.

[18] In both June and August, tracer penetration was observed at greater depths in AS compared to PS with a 1.01 m maximum occurring in August. The maximum depth of tracer observed in the peat-lined reach was 0.15 m during the June SIE. Additionally, the observed mean arrival times, t_{MEDOBS}, beneath AS were generally much shorter (1980–9306 s) than beneath PS (8370–19,458 s) (Table S1).

3.2. Hyporheic Exchange Modeling

[19] For both AS SIEs, the highest K_X values were found in the riffle tail K zones (0.020 and 0.023 m s^{-1}, in June and August respectively, Table S2) and the lowest K_X values were identified for the pool zones (0.006 and 0.011 m s^{-1}, in June and August respectively). In PS, the highest K_X values were simulated for the run zones (0.0045 m s^{-1} for both June and August), while the pool zone K_X were the lowest (0.004 and 0.003 m s^{-1}, in June and August respectively). Accordingly, the greatest t_{MEDSIM} (21,062 s) occurred at a PS pool sampler, and the lowest t_{MEDSIM} (1092 s) occurred at an AS riffle head sampler (Table S1).

[20] The forward MODPATH simulations for both sites represent 10 days (864,000 s) of particle transport time. The longitudinal hyporheic flowpaths for AS were longer and more continuous across the length of the reach than those in PS (Figure 1). The AS flowpaths primarily deepened with increased thaw depth. However, with deepening flowpaths, some flowpaths also elongated (e.g., between June and August AS simulations some flowpaths elongated as much as 74.5 m). In the peat-lined reach, minor elongation of
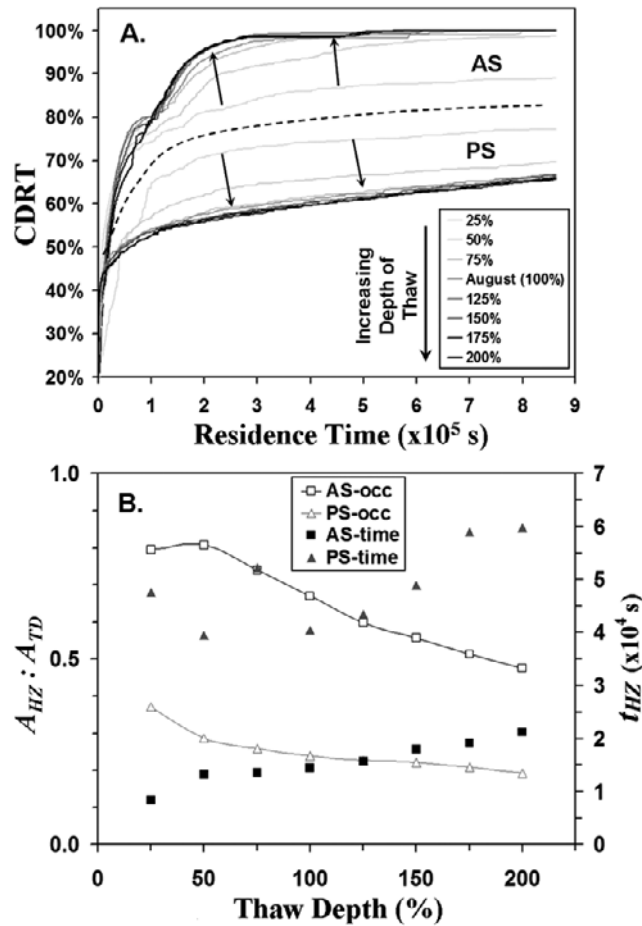
Figure 2. (a) Cumulative distribution of residence times (CDRTs) of simulated hyporheic particle for thaw scenarios in the alluvial reach (AS) and peat-lined reach (PS). (b) Comparison of inter-scenario and -site median simulated hyporheic residence time for all reach particles, t_{HZ} ("time" labeled values), and evaluations of simulated hyporheic occupation ("occ" labeled values, the ratio of A_{HZ} to A_{TD} as defined in section 2.3).

hyporheic flowpaths occurs as a result of deeper penetration in the August model (Figure 1). Additionally, the majority of the simulated flowpaths in PS for both models were located at the top of the reach and at run locations where heads decreased longitudinally. Hydraulic head gradients were more varied along AS than PS. The deepest hyporheic flowpaths mimic the topography of the thaw extent. Where the hydraulic head gradient was sufficient, some flowpaths in all simulations penetrated the full thickness of the thawed subsurface.

[21] The simulated CDRTs are very different between the two reaches for the June and August forward simulations. Of the particles released in the June AS model, 98.4% were simulated to return to surface flow or pass out of the bottom of the reach (i.e., boundary conditions set to capture released particles), and all particles returned to the stream in the August model (Figure 2). However, only 71.5 and 66.8% of the hyporheic particles for June and August PS models, respectively, return to the stream within the 10 day simulation. The unaccounted for hyporheic particles were

those still in the subsurface at the end of the simulation. The median simulated hyporheic residence time for all particles in a reach, t_{HZ}, was also calculated. In PS, the August t_{HZ} value was $\sim 3\times$ greater than the June t_{HZ} value (40,440 and 14,700 s, respectively). However, the AS t_{HZ} values were comparable between June and August simulations (20,280 and 14,460 s, respectively).

[22] Across the broader range of thaw depths, the value of t_{HZ} increased with thaw thickness in the AS reach but decreased in the PS reach with greater thaw (Figure 2). The CDRTs for each thaw scenario, show that the AS late-time distribution continued to account for larger portions of the simulated particle residence times as the thaw increased from 25 to 200% of the August thickness. However, for the 125–200% thaw depth scenarios in AS, the cumulative percentage of particles with residence times >10,000 s did not differ significantly. Likewise, the CDRTs of PS collapse upon one another, but across a broader range of thaw depths (100 to 200%). Additionally, the PS CDRTs differ less at times <10,000 s than in AS. Independent of the thaw thickness, approximately half of the simulated particle transport times are <68,700 s in PS, while in AS the same proportion of particles had transport times <22,080 s. Furthermore, all simulations with greater than 75% thaw in AS had particle residence times <10 d (i.e., all particles captured). There were no PS scenarios where all particles had residence times <10 d. The greatest percentage of particles captured in PS occurred at the shallowest thaw scenario (25% thickness).

[23] The spatial analysis of simulated flowpaths for each site showed that the relative shifts in $A_{HZ}*$ were similar for thaw scenarios 150 to 200% (Figure 2). However, $A_{HZ}*$ values for the AS reach had a larger range of inter-scenario variation for simulations up to 150% thaw. Between sites, hyporheic occupation (i.e., $A_{HZ}:A_{TD}$) of the AS thawed depth was much greater than that of the PS reach, ranging from 0.48 for the 200% scenario up to 0.81 for the 50% thaw scenario (Figure 2). The PS hyporheic occupation ranged from 0.19–0.37 (200% and 25% thaw scenario, respectively).

4. Discussion and Conclusions

[24] At 100% thaw depth condition in August, the PS hyporheic flowpaths and transport rates are not limited by permafrost. When the morphologic and surface water characteristics are held constant, differences in thaw depth had a limited effect on the hyporheic flow conditions. In all thaw thickness scenarios beyond the conditions observed in August, there was little change in the CDRT shape and the portion of thaw occupied by hyporheic exchange (Figure 2). Low-energy, peat-lined streams of the Arctic have hyporheic zones that are morphology-limited throughout most of the year (i.e., the extent of hyporheic flow is limited by the hydraulic gradients established by surface flows, longitudinal bed topography, and sediment K values).

[25] In the AS reach we observed that across thaw scenarios the majority of the residence times increase with greater thaw and that a portion of the flowpaths maintain an interface with the permafrost boundary, which suggests that permafrost might limit hyporheic dynamics in some cases. However, in both the PS and AS reaches, the rates of

change in hyporheic residence time and extent begin to diminish and become asymptotic under most of the thicker thaw scenarios. For AS, this active-layer condition occurs at approximately 125% of the August thaw thickness as shown by the collapse of the CDRTs onto one distribution and the minimal rate of change for t_{HZ} and $A_{HZ}:A_{TD}$ for conditions beyond 125% (Figure 2). The same threshold observations were made for PS, but they occurred at the 75% thaw scenario. Both streams were similar in that across thaw thicknesses, most of the exchange occurs at relatively short residence times. This is consistent with simulations of hyporheic exchange in both smaller [*Wroblicky et al.*, 1998] and larger [*Saenger et al.*, 2005] streams. The difference between the two stream hyporheic particle recoveries (Figure 2) is a result of the different hydraulic and permafrost properties of each stream system. For example, relative to AS, fewer particles are recovered over the simulation period in PS because particle transport times are increased by the low K values, weak hydraulic head gradients, and tortuous flowpaths created by a irregular permafrost boundary geometry.

[26] These two streams represent end-members along a permafrost-hyporheic continuum that is bounded by the extremes of morphology-limited and permafrost-limited systems. Within this continuum, most streams will be operating under both limitations, but at different periods and durations of the thaw season. As reported by *Brosten et al.* [2006] and *Zarnetske et al.* [2007], the mean thaw thickness under most headwater streams in the Arctic increases very rapidly at the beginning of the thaw season and appears to reach a stable thickness that persists throughout the majority of the thaw period. In all stream cases, this stable depth was achieved by August. Thus, the conditions we observed in August likely represent the near-equilibrium state created under the balance of prevailing surface flow, bed morphology, and permafrost conditions, as evidenced by the minor changes in the CDRTs at 100%+ thaw scenarios (Figure 2).

[27] This investigation illustrates that morphologic and hydraulic conditions (i.e., surface and groundwater flow properties) set the potential for hyporheic flow, and that no-flow conditions such as permafrost (or similarly, shallow subsurface bedrock or very low conductivity sediments) can constrain this hyporheic flow potential. The modeling also indicates that, if the established hyporheic flow conditions are insufficient to create an interface with an underlying no-flow condition and there is no influence from a larger groundwater aquifer, the hyporheic exchange will be independent of the no-flow features.

[28] Ultimately, to best predict the implications of a warming climate on hyporheic exchange in streams underlain by permafrost, we will need to forecast how the morphology of the channels will adjust to the climate driven perturbations. This understanding is beyond the scope of this investigation. However, in the absence of this complete understanding, we have established that without changes to the stream surface morphology, a deepening subsurface thaw will only affect hyporheic exchange until a threshold depth is achieved, and that this depth is primarily determined by the hydraulic head gradients imposed by the dominant morphology of the stream.

References

Best, H., J. McNamara, and L. Liberty (2005), Association of ice and river channel morphology determined using ground penetrating radar in the Kuparuk River, Alaska, *Arct. Antarct. Alp. Res.*, 37(2), 157–162.

Bradford, J., J. McNamara, W. Bowden, and M. Gooseff (2005), Imaging depth-of-thaw beneath arctic streams using ground-penetrating radar, *Hydrol. Processes*, 19, 2689–2699.

Brosten, T., J. Bradford, J. McNamara, J. Zarnetske, M. Gooseff, and W. Bowden (2006), Profiles of temporal thaw depths beneath two arctic stream types using ground-penetrating radar, *Permafrost Periglacial Processes*, 17, 341–355.

Edwardson, K., W. Bowden, C. Dahm, and J. Morrice (2003), The hydraulic characteristics and geochemistry of hyporheic and parafluvial zones in arctic tundra streams, North Slope, Alaska, *Adv. Water Resour.*, 26, 907–923.

Freeze, R., and J. Cherry (1979), *Groundwater*, Prentice-Hall, Upper Saddle River, N. J.

Greenwald, M. (2007), Hyporheic exchange and biogeochemical processing in arctic tundra streams, M.Sc. thesis, Univ. of Vt., Burlington.

Haggerty, R., S. M. Wondzell, and M. A. Johnson (2002), Power-law residence time distribution in the hyporheic zone of a 2nd-order mountain stream, *Geophys. Res. Lett.*, 29(13), 1640, doi:10.1029/2002GL014743.

Harvey, J., and K. Bencala (1993), The effect of streambed topography on surface-subsurface water exchange in mountain catchments, *Water Resour. Res.*, 29, 89–98.

Jones, J., and P. Mulholland (Eds.) (2000), *Streams and Groundwaters*, Academic, San Diego, Calif.

Kasahara, T., and S. M. Wondzell (2003), Geomorphic controls on hyporheic exchange flow in mountain streams, *Water Resour. Res.*, 39(1), 1005, doi:10.1029/2002WR001386.

Osterkamp, T., and V. Romanovsky (1999), Evidence for warming and thawing of discontinuous permafrost in Alaska, *Permafrost Periglacial Processes*, 10, 17–37.

Saenger, N., P. K. Kitanidis, and R. L. Street (2005), A numerical study of surface-subsurface exchange processes at a riffle-pool pair in the Lahn River, Germany, *Water Resour. Res.*, 41, W12424, doi:10.1029/2004WR003875.

Wroblicky, G., M. Campana, H. Valett, and C. Dahm (1998), Seasonal variation in surface-subsurface water exchange and lateral hyporheic area of two stream-aquifer systems, *Water Resour. Res.*, 34, 317–328.

Zarnetske, J. P., M. N. Gooseff, T. R. Brosten, J. H. Bradford, J. P. McNamara, and W. B. Bowden (2007), Transient storage as a function of geomorphology, discharge, and permafrost active layer conditions in Arctic tundra streams, *Water Resour. Res.*, 43, W07410, doi:10.1029/2005WR004816.

———————————

W. B. Bowden and M. J. Greenwald, Rubenstein School of the Environment and Natural Resources, University of Vermont, 304 Aiken Center, Burlington, VT 05405, USA.

J. H. Bradford, T. R. Brosten, and J. P. McNamara, Department of Geosciences, Boise State University, 1910 University Drive, Boise, ID 83729, USA.

M. N. Gooseff, Department of Civil and Environmental Engineering, Pennsylvania State University, 212 Sackett Building, University Park, PA 16802, USA.

J. P. Zarnetske, Department of Geosciences, Oregon State University, 104 Wilkinson Hall, Corvallis, OR 97331, USA. (zarnetsj@geo.oregonstate.edu)